Semarak International Journal of
Fundamental and Applied Mathematics

Journal homepage:
https://semarakilmu.my/index.php/sijfam/index
ISSN: 3030-5527

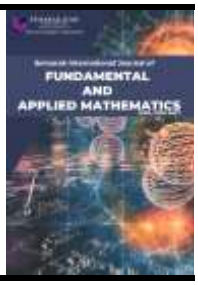

Numerical Computations Arising from Time-Memory Partial Integro-Differential Equations

Okey Oseloka Onyejekwe[1,*]

[1] Robnello Unit for Continuum Mechanics and Nonlinear Dynamics, Ishiagu Oshimili South Asaba, Delta State Nigeria

ARTICLE INFO

Article history:
Received 25 March 2025
Received in revised form 29 April 2025
Accepted 22 May 2025
Available online 30 June 2025

Keywords:
Time-memory; partial integro-differential equation; quadrature, numerical scheme; nonlinear algebraic equations

ABSTRACT

In the work reported herein, numerical solutions of a memory-type generalized Fisher-integro-differential equation is presented. A composite weighted trapezoidal rule is manipulated to handle the numerical integration and the governing partial differential equation is converted to a system of nonlinear algebraic equations. These procedures are explained in detail and solved straightforwardly. Different types of boundary conditions are examined; including the non-trivial Robin types. Accuracy properties of the numerical scheme are confirmed by comparing the numerical results with analytical solutions obtained from literature.

1. Introduction

The addition of a memory component into a partial differential equation defines an evolution equation that combines differential and integral operators. Such an equation otherwise known as a partial integro-differential equation (PIDE) is used to describe complicated systems where the rate of change of a scalar variable depends on its past and present values. It has an enormous application in various fields of science. For instance, PIDEs are used to model transport phenomena in such diverse areas as biomedical engineering [1], economics [2], population [3], heat and mass transfer [4], reaction-transport systems [5].

They have proven to be reliable especially in addressing cases where the determination of a scalar profile requires information from a preceding time interval. For example, a standard heat equation assumes a constant diffusion coefficient and instantaneous response to concentration. This cannot be valid especially for non-homogeneous media or high viscosity fluids conditioned by their complex internal structure. For example, a particle transported in a cellular environment is influenced by a non-constant or time dependent diffusivity. This is also relevant in social network where past

* *Corresponding author.*
E-mail address: okuzaks@yahoo.com

https://doi.org/10.37934/sijfam.6.1.1427

opinions or exposures for example 'fake news' can affect subsequent response via a diffusion process.

Scientific literature is replete with information leading to different methods for the study of these type of equations. These include finite difference (FD), spectral and collocation techniques [6-20]. Continuous and discrete models have been applied to describe reaction transport systems with long range and memory interactions designed to achieve thermal efficiencies Ferreira and Pinto [21]. H eat equation with memory was further explored by Branco and Ferreira [22] by using the multiplier method and a general lemma about convergent and divergent series. Their study considered the hyperbolic equation as a singular perturbation of the heat equation with memory within the context of decay of solutions. A comprehensive treatment of finite difference (FD) based solutions of time-memory diffusion can be found in [23].

Basically, two important variables come into play, namely the proportionality of a flux gradient accompanied by the distribution of a scalar variable. This idea finds relevance in several fields such as in the case of momentum flux caused by velocity gradients, in heat flux giving rise to temperature gradients or in an electric current caused by an electric field. The introduction of a 'memory' term component in an integro-differential equation is an attempt to address an unphysical infinite propagation velocity that accompanies the appearance of flux at the onset of a gradient [21]. This has continued to be an active area of scientific research [6-20]. A good many of the numerical techniques applied to address this challenge often involves rigorous numerical techniques that do not guarantee straightforward application. Quite often the mathematical rigor alone obfuscates the physics of the problem.

We address this concern by deliberately introducing an FD based method that is accurate, flexible and inexpensive. Problems with closed form solution taken from literature were used for comparison, and in all cases very accurate results were obtained in their overall analysis.

The integro-differential equation to be discussed herein, represents a Fisher-type prototypical reaction-diffusion equation that includes the derivatives and the integration of the unknown function together with independent variables. Equations of this type have found application in various branches of science and engineering. A typical challenge encountered here is the numerical complication from both the nonlinearity and the integral component of the governing equation. To prevail over this problem Araujo *et al*.[24] , took into account the boundness of the transport process by introducing a relaxation parameter τ which represents the waiting time between two successive jumps of the particles whose movement we want to determine.

In this paper, we adopt a numerical method based on a finite difference technique for dealing with both the derivative and an integral component of equation (1) in a straightforward manner. We obviate the numerical challenges encountered in the numerical solution especially in the resolution of the memory component by modifying the technique proposed by [24].

2. Problem Formulation

The governing differential equation for this work can be represented as:

$$u_t = q(x,t) + f(u) + \lambda u_x + \mu u_{xx} + \frac{D}{\tau}\int_0^t e^{-(t-s)/\tau} u_{xx} ds \tag{1}$$

The initial and boundary conditions can generally be put in the form:

$$u(x,0)=p(x),\quad x\in[a,b]$$
$$\alpha_0 u(a,t)+\beta_0 u_x(a,t)=b_0(t);\ t\in[0,T]$$
$$\alpha_1 u(b,t)+\beta_1 u_x(b,t)=b_1(t);t\in[0,T]$$

where $u(x,t)$ is the unknown function; $u_t=\partial u/\partial t,\ u_{xx}=\partial^2 u/\partial x^2$ are the transient and diffusion terms. τ, the relaxation parameter, $q(x,t),\ p(x),b_0(t),b_1(t)$ are prescribed functions which are continuous on the problem domain Ω. In addition, $\alpha_0,\alpha_1,\ \beta_0,\beta_1,\lambda,\mu,D,and\ \tau$ are given constants and $f(u)$ is a given function of the dependent variable or simply the reaction term.

Consider nodal points (x_k,t_k) defined within a problem domain $[a,b]\times[0,T]$,

$$\text{where } a=x_1<x_2<.....x_M<x_{M+1}=b,\ x_{i+1}-x_i=\Delta x,$$
$$\text{and } 0=t_1<t_2<.....t_N<t_{N+1}=T,\ t_{k+1}-t_k=\Delta t$$

In a typical discrete representation of the space and time domains:

$$x_i=a+(i-1)\Delta x\ \ for\ i=1,2....M+1,$$
$$\text{and } t_k=(k-1)\Delta t,\ k=1,2,...N+1$$

A weighted trapezoidal rule is used to approximate the integral term.

$$\int_{t_1}^{t_{N+1}} g(s)ds\approx\frac{\Delta t}{2}\sum_{k=1}^{N}\left[g(t_k)+g(t_{k+1})\right] \tag{2}$$

Hence, the diffusive integral kernel term is discretized as:

$$\int_0^{t_{N+1}} e^{-\frac{t_{N+1-s}}{\tau}}u_{xx(x,s)}ds\approx \tag{3}$$
$$\frac{\Delta t}{2}\sum_{k=1}^{N}\left[e^{-\frac{t_{N+1}-t_k}{\tau}}u_{xx(x,t_k)}+e^{-\frac{t_{N+1}-t_{k+1}}{\tau}}u_{xx(x,t_{k+1})}\right]$$

A Taylor series central difference scheme is used for the flux or derivative term

$$u_x(i,k)=\frac{u(i+1,k)-u(i-1,k)}{2\Delta x} \tag{4}$$

The boundary conditions, can be Dirichlet, Neumann or Robin. However, for the special case of the Robin; the discretization involving the boundary nodes $(x=a,\ x=b)$ corresponding to $i=1\ and\ i=M+1$ nodes respectively for M number of nodal spaces, are represented for the first and last nodes as:

$$\alpha_o u\left(x_1,t_k\right)+\beta_0\left[\frac{u\left(x_2,t_k\right)-u\left(x_0,t_k\right)}{2\Delta x}\right]=b_0\left(t_k\right) \tag{5}$$

$$\alpha_1 u\left(x_{M+1},t_k\right)+\beta_1\left[\frac{u\left(x_{M+2},t_k\right)-u\left(x_M,t_k\right)}{2\Delta x}\right]= \ b_1\left(t_k\right) \tag{6}$$

Eqs. (5) and (6) can be put in an easily computable form to read:

$$u\left(x_0,t_k\right)=\frac{1}{\beta_0}\left[\beta_0 u\left(x_2,t_k\right)+2\Delta x\alpha_0 u\left(x_1,t_k\right)-2\Delta x b_0\left(t_k\right)\right] \tag{7}$$

$$u\left(x_{M+2},t_k\right)= \ \frac{1}{\beta_1}\left[\beta_1 u\left(x_M,t_k\right)+2\Delta x\alpha_1 u\left(x_{M+1},t_k\right)-2\Delta x b_1\left(t_k\right)\right] \tag{8}$$

The above discretization stencils facilitate the application of a Crank-Nicolson (C-N) type scheme to the governing differential equation (equation (1.)) and is given as:

$$\begin{aligned}&\frac{\left(u_i^{k+1}-u_i^k\right)}{\Delta t}=q_i^k+\frac{1}{2}\left[\left(f\left(u\right)\right)_i^k+\left(f\left(u\right)\right)_i^{k+1}\right]+\frac{\lambda}{4\Delta x}\left[u_{i+1}^k-u_{i-1}^k+u_{i+1}^{k+1}-u_{i-1}^{k+1}\right]+\\&\frac{\mu}{2\Delta x^2}\left[u_{i-1}^k-2u_i^k+u_{i+1}^k+u_{i-1}^{k+1}-2u_i^{k+1}+u_{i+1}^{k+1}\right]+\frac{D\Delta t}{2\tau\Delta x^2}\sum_{k=1}^{N}e^{-\frac{t(N+1)-t(k+1)}{\tau}}\left[u_{i+1}^{k+1}-2u_i^{k+1}-u_{i-1}^{k+1}\right]\end{aligned} \tag{9}$$

If the reaction function $f\left(u\right)$ is nonlinear, it can be linearized via the Taylor series expansion as:

$$\left(f\left(u\right)\right)_i^{k+1}\approx\left(f\left(u\right)\right)_i^k+\Delta t\left(\frac{\partial f\left(u\right)}{\partial t}\right)_i^k=\left(\frac{\partial f\left(u\right)}{\partial u}\right)\left(\frac{\partial\left(u\right)}{\partial t}\right)=\Delta t\left(\frac{\partial f\left(u\right)}{\partial u}\right)\left(u_i^{k+1}-u_i^k\right) \tag{10}$$

Eq. (9) can be factorized to read:

$$\begin{aligned}&\left[\frac{\lambda Dt}{4\Delta x}-\frac{\mu\Delta t}{2\Delta x^2}-\frac{D\Delta t^2}{2\tau\Delta x^2}\sum_{k-1}^{N}e^{-\frac{t(N+1)-t(k+1)}{\tau}}\right]u_{i-1}^{k+1}+\left[1-\frac{\Delta t}{2}\left(\frac{\partial f\left(u\right)}{\partial u}\right)_i^k+\frac{\mu\Delta t}{\Delta x^2}+\frac{D\Delta t^2}{2\tau\Delta x^2}\sum_{k-1}^{N}e^{-\frac{t(N+1)-t(k+1)}{\tau}}\right]u_i^{k+1}+\\&\left[\frac{\lambda Dt}{4\Delta x}+\frac{\mu\Delta t}{2\Delta x^2}+\frac{D\Delta t^2}{2\tau\Delta x^2}\sum_{k-1}^{N}e^{-\frac{t(N+1)-t(k+1)}{\tau}}\right]u_{i+1}^{k+1}=\\&\left[-\frac{\lambda Dt}{4\Delta x}+\frac{\mu\Delta t}{2\Delta x^2}+\frac{D\Delta t^2}{2\tau\Delta x^2}\sum_{k-1}^{N}e^{-\frac{t(N+1)-t(k+1)}{\tau}}\right]u_{i-1}^{k}+\left[1-\frac{\Delta t}{2}\left(\frac{\partial f\left(u\right)}{\partial u}\right)_i^k-\frac{\mu\Delta t}{\Delta x^2}-\frac{D\Delta t^2}{2\tau\Delta x^2}\sum_{k-1}^{N}e^{-\frac{t(N+1)-t(k+1)}{\tau}}\right]u_i^{k}+\\&\left[\frac{\lambda Dt}{4\Delta x}+\frac{\mu\Delta t}{2\Delta x^2}+\frac{D\Delta t^2}{2\tau\Delta x^2}\sum_{k-1}^{N}e^{-\frac{t(N+1)-t(k+1)}{\tau}}\right]u_{i+1}^{k}+\ \Delta tq_i^k+\Delta t\left(f\left(u\right)\right)_i^k\end{aligned} \tag{11}$$

Further simplification leads to a tri-diagonal matrix form. Subsequently, the following time evolution equation is solved for each node:

$$\left[\frac{\lambda\Delta t}{4\Delta x}-\frac{\mu\Delta t}{2D\Delta x^2}-\frac{D\Delta t^2}{2\tau\Delta x^2}e^{-\frac{t(N+1)-t(k+1)}{\tau}}\right]u_{i-1}^{k+1}+\left[1-\frac{\Delta t}{2}\left(\frac{\partial f(u)}{\partial u}\right)_i^k+\frac{\mu\Delta t}{2\Delta x^2}+\frac{D\Delta t^2}{\tau\Delta x^2}e^{-\frac{t(N+1)-t(k+1)}{\tau}}\right]u_i^{k+1}$$
$$-\left[\frac{\lambda\Delta t}{4\Delta x}+\frac{\mu\Delta t}{2D\Delta x^2}+\frac{D\Delta t^2}{2\tau\Delta x^2}e^{-\frac{t(N+1)-t(k+1)}{\tau}}\right]u_{i+1}^{k+1}=$$
$$\left[-\frac{\lambda\Delta t}{4\Delta x}+\frac{\mu\Delta t}{2D\Delta x^2}+\frac{D\Delta t^2}{2\tau\Delta x^2}e^{-\frac{t(N+1)-t(k+1)}{\tau}}\right]u_{i-1}^{k}+\left[1-\frac{\Delta t}{2}\left(\frac{\partial f(u)}{\partial u}\right)_i^k-\frac{\mu\Delta t}{2\Delta x^2}-\frac{D\Delta t^2}{\tau\Delta x^2}e^{-\frac{t(N+1)-t(k+1)}{\tau}}\right]u_i^{k}$$
$$+\left[\frac{\lambda\Delta t}{4\Delta x}+\frac{\mu\Delta t}{2D\Delta x^2}+\frac{D\Delta t^2}{2\tau\Delta x^2}e^{-\frac{t(N+1)-t(k+1)}{\tau}}\right]u_{i+1}^{k} \tag{12}$$

Eq. (12) is put in a compact form to read:

$$(z_2-z_1-z)u_{i-1}^{k+1}+\left(1-0.5\Delta t\left(\frac{\partial f(u)}{\partial u}\right)_i^k+2z+2z_1\right)u_i^{k+1}-(z_2+z_1+z)u_{i+1}^{k+1}=$$
$$(-z_2+z_1+z_3)u_{i-1}^{k+1}+\left(1-0.5\Delta t\left(\frac{\partial f(u)}{\partial u}\right)_i^k-2z_1-2z_3\right)u_i^{k}+(z_2+z_1+z_3)u_{i+1}^{k}+\Delta t q_i^k+\Delta t\left(f(u)\right)_i^k \tag{13}$$

where

$$z=\frac{D\Delta t^2}{2\tau\Delta x^2}e^{-\frac{t(N+1)-t(k+1)}{\tau}},\quad z_1=\frac{\mu\Delta t}{2\Delta x^2},\quad z_2=\frac{\lambda\Delta t}{4\Delta x},\quad z_3=\frac{D\Delta t^2}{2\tau\Delta x^2}e^{-\frac{t(N+1)-t(k)}{\tau}}$$

The final form of Eq. (13) depends on the specified boundary conditions on the first and the last nodes $\left(u_1^{k+1}, u_{M+1}^{k+1}\right)$. For the Dirichlet boundary conditions both the coefficient matrix and the right-hand side (RHS) vector should be configured to yield the specified values at the terminal nodes as shown in Figure 1.

$$\begin{bmatrix} a & -b & 0 & 0 & 0 & . & . & . & 0 \\ c & a & -b & 0 & 0 & 0 & . & . & 0 \\ 0 & c & a & -b & 0 & . & . & . & 0 \\ . & . & . & . & . & . & . & . & . \\ . & . & . & . & . & . & . & . & . \\ . & . & . & . & . & . & . & . & . \\ 0 & 0 & & & & c & a & -b & 0 \\ 0 & 0 & . & . & . & 0 & c & a & -b \\ 0 & 0 & 0 & 0 & 0 & 0 & 0 & c & a \end{bmatrix}\begin{vmatrix} u_2^{k+1} \\ u_3^{k+1} \\ 0 \\ 0 \\ . \\ . \\ u_{M-2}^{k+1} \\ u_{M-1}^{k+1} \\ u_M^{k+1} \end{vmatrix}=\begin{vmatrix} -cu_1^{k+1}+D_2 \\ D_3 \\ D_4 \\ . \\ . \\ . \\ D_{M-2} \\ D_{M-1} \\ -cu_M^{k+1}+D_M \end{vmatrix}$$

Fig. 1. Matrix stencil for Dirichlet boundary condition

where a, c are the coefficients of u_{i-1}^{k+1}, u_i^{k+1}, u_{i+1}^{k+1} respectively.

On the other hand, both the derivative-related boundary conditions (Robin and Neumann) depend on the solution. Without any loss in generality we construct the solution matrix equation for the Robin boundary condition to yield (see Figure 2):

$$\begin{bmatrix} c_1 & c-b & 0 & 0 & 0 & . & . & . & 0 \\ c & a & -b & 0 & 0 & 0 & . & . & 0 \\ 0 & c & a & -b & 0 & . & . & . & 0 \\ . & . & . & . & . & . & . & . & . \\ . & . & . & . & . & . & . & . & . \\ . & . & . & . & . & . & . & . & . \\ 0 & 0 & 0 & 0 & 0 & c & a & -b & 0 \\ 0 & 0 & . & . & . & 0 & c & a & -b \\ 0 & 0 & 0 & 0 & 0 & 0 & 0 & c-b & c_2 \end{bmatrix} \begin{vmatrix} u_1^{k+1} \\ u_2^{k+1} \\ u_3^{k+1} \\ . \\ . \\ . \\ u_{M-1}^{k+1} \\ u_M^{k+1} \\ u_{M+1}^{k+1} \end{vmatrix} = \begin{vmatrix} a_1 + D_1 \\ D_2 \\ D_3 \\ . \\ . \\ . \\ D_{M-1} \\ D_M \\ a_2 + D_{M+1} \end{vmatrix}$$

Fig. 2. Matrix stencil for Robin boundary condition

The following substitutions hold for the first and last nodes.

$$\text{for } i = 1 \ (\text{first node}) \tag{14}$$
$$\left(a + \frac{2c\alpha_0 \Delta x}{\beta_0}\right) u_1^{k+1} + (c-b) u_2^{k+1} = D_1 + \frac{2c\Delta x}{\beta_0} b_0 \left(t(k+1)\right)$$

$$\text{for} \quad i = M+1 \ (\text{last node}) \tag{15}$$
$$(c-b) u_M^{k+1} + \left(a + \frac{2b\alpha_1 \Delta x}{\beta_1}\right) u_{M+1}^{k+1} = D_{M+1} + \frac{2b\Delta x}{\beta_1} b_1 \left(t(k+1)\right)$$

where

$$D_i = (z_1 - z_2 + z_3) u_{i-1}^k + \left(1 - \frac{\Delta t}{2}\left(\frac{\partial f(u)}{\partial u}\right)_i^k - 2z_1 - 2z_3\right) u_i^k + (z_1 + z_2 + z_3) u_{i+1}^k + \Delta t q_i^k + \Delta t \left(f(u)\right)_i^k$$

$$c = (z_2 - z_1 - z), \ a = 1 - \frac{\Delta t}{2}\left(\frac{\partial f(u)}{\partial u}\right)_i^k + 2z + 2z_1, \ b = z_2 + z_1 + z \ , c_1 = a + \frac{2c\alpha_0 \Delta x}{\beta_0}, \ c_2 = a + \frac{2b\alpha_1 \Delta x}{\beta_1},$$

$$a_1 = \frac{2c\Delta x}{\beta_0} b_0 \left(t(k+1)\right), a_2 = \frac{2b\Delta x}{\beta_1} b_1 \left(t(k+1)\right)$$

3. Numerical Experiments

Four examples are presented to support the utility of this method. Two of them come with analytic solutions while for the remaining the exact solutions are unknown. The transient numerical solutions for all the examples are plotted to demonstrate the time evolution of the profiles; and

where the analytic solution exists, the absolute error is chosen as a means of ascertaining the error associated with the numerical computations. These examples are solved using MATLAB

2.1 Example 1

Consider IPDE with a nonlinear reaction term

$$u_t = u^2 - \frac{1}{2\pi^2}u_{xx} + \int_0^t e^{-(t-s)/\tau}u_{xx}(x,s)\,ds + q(x,t) \tag{16}$$
$$q(x,t) = \pi^2 te^{-t}\sin(\pi x) - e^{-t}\sin^2(\pi x)$$

Initial condition is:

$$u(x,0) = \sin(\pi x)$$

Robin-type boundary conditions are specified as:

$$u(0,t) + u_x(0,t) = \pi e^{-(t/2)}$$
$$u(1,t) + u_x(1,t) = -\pi e^{-(t/2)}$$

The analytic solution is given as:

$u(x,t) = e^{-(t/2)}\sin(\pi x)$ [15]

The problem is solved with a step size, $\Delta x = .02$, and time step $\Delta t = .001$. Figures 3 and 4 show the plots of the numerical solutions at different time levels as well as the absolute errors. Figure 3 bears an excellent agreement with the diagram displayed in [15] for the solution of the same problem.

The magnitude of the absolute errors is highest in areas corresponding to those with the highest gradients in Figure 3 and decreases significantly on both sides of Figure 4. On the whole the magnitude of the absolute error shows a downward trend.

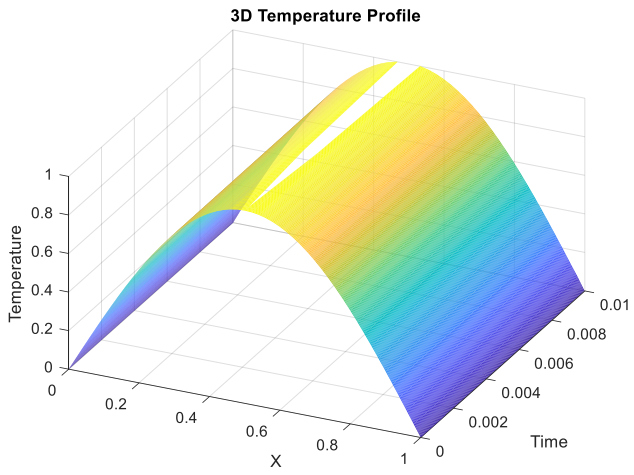

Fig. 3. 3D Temperature profiles for Example 1

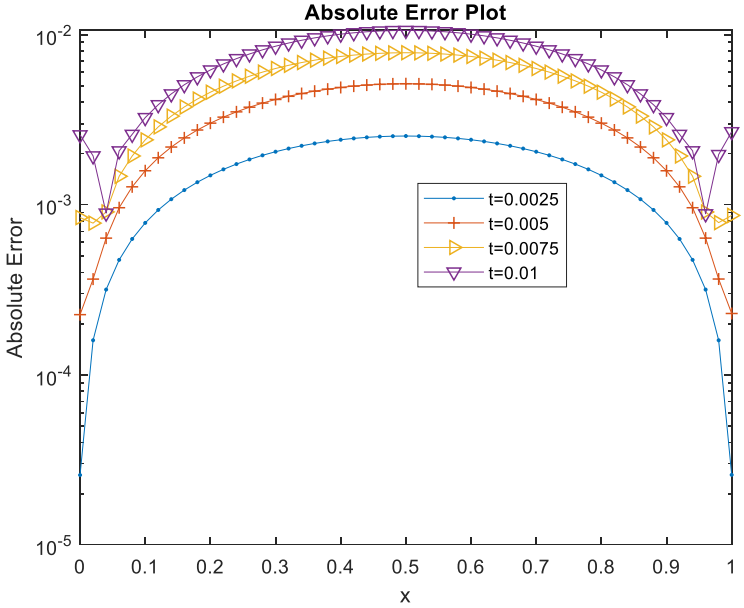

Fig. 4. Absolute errors for Example 1

2.2 Example 2

Here, modifications to the previous IPDE to read:

$$u_t = u^2 + \frac{1}{2\pi^2}u_{xx} + \int_0^t e^{-(t-s)/\tau}\, u_{xx}\, ds + q(x,t)\, ds \tag{17}$$

where $(x,t)\in(0,1)\times(0,1]$.

The nonlinear reaction term remains the same, but the initial condition, the source term and the exact solution are all piecewise continuous.

Initial condition:

$u(x,0)=\begin{cases}\sin(\pi x) & 0\le x\le 0.5\\ 1 & 0.5\le x\le 1\end{cases}$ and boundary conditions $u(0,\mathrm{t})=0,\quad u(1,t)=e^{-(t)/2}$. The source term is given as

$$q(x,\mathrm{t})=\begin{cases}\pi^2 te^{-t/2}\sin(\pi x)-e^{-t}\sin^2(\pi x) & 0\le x\le 0.5\\ -1 & 0.5\le x\le 1.0\end{cases}$$

And the exact solution:

$$q(x,\mathrm{t})=\begin{cases}e^{-t/2}\sin^2(\pi x) & 0\le x\le 0.5\\ e^{-t/2} & 0.5\le x\le 1.0\end{cases}$$

Unless expressed otherwise both the time and spatial step sizes remain the same.

Figures 5, 6 and 7 display various aspects of the solution profiles at different time levels. Figure 5 shows the shape of the numerical solution profiles as they evolve with time. The profiles of absolute errors at specific time periods are displayed in Figure 6. There is an overall downward trend as the computation proceeds. A 3D picture of the transient profiles is shown in Figure 7. This is in agreement with the profile shown in [15] for the solution of the same problem.

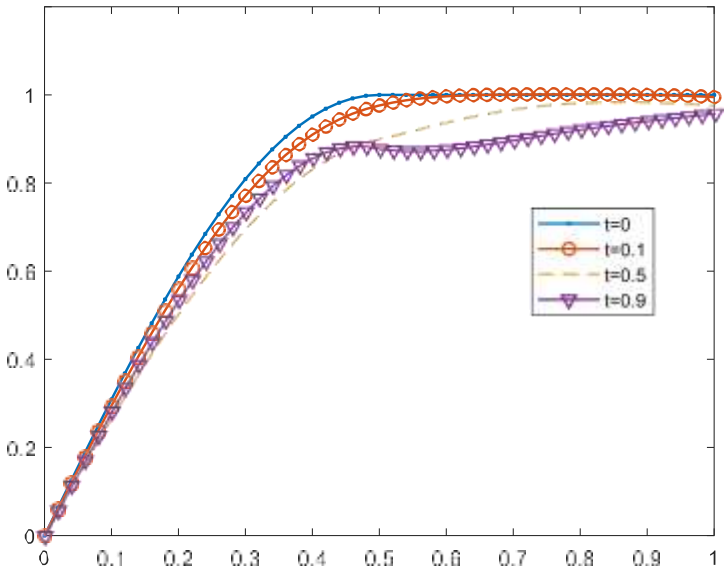

Fig. 5. Time evolution of solution profiles for Example 2

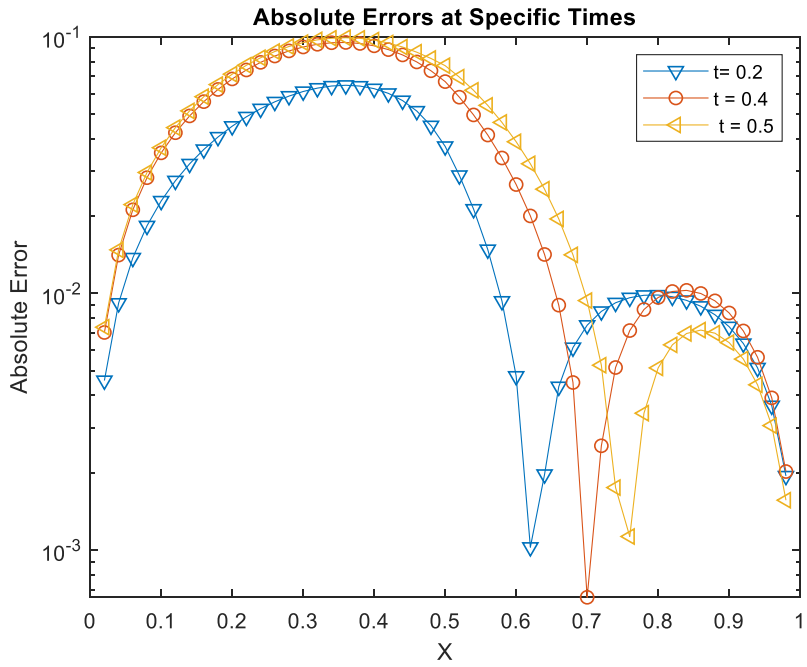

Fig. 6. Magnitude of absolute errors at different time periods for Example 2

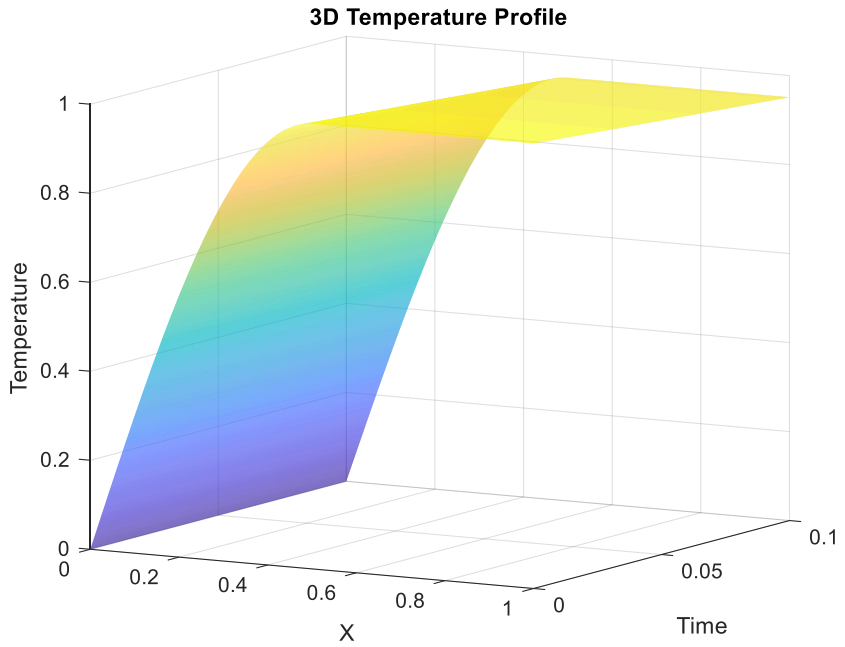

Fig. 7. 3D temperature profiles for Example 2

2.3 Example 3

We consider the following IPDE for our third example.

$$u_t = u(1-u) - 0.5u_x + 0.1u_{xx} + 10\int_0^t e^{-(t-s)/0.01}\, u_{xx}\, ds \tag{18}$$

where $(x,t)\in(0,10)\times(0,10]$.The following initial and boundary conditions apply:

$$u(x,0)=\begin{cases}1, & 0\le x\le 5\\ 0, & 5\le x\le 10\end{cases}$$

Boundary conditions: $u(0,t)=1, \quad u(10,t)=0$.

Figures 8 and 9 are time evolution profiles of a problem whose analytical solution is not given. They are consistent with those displayed in [15] and [24] for an identical problem.

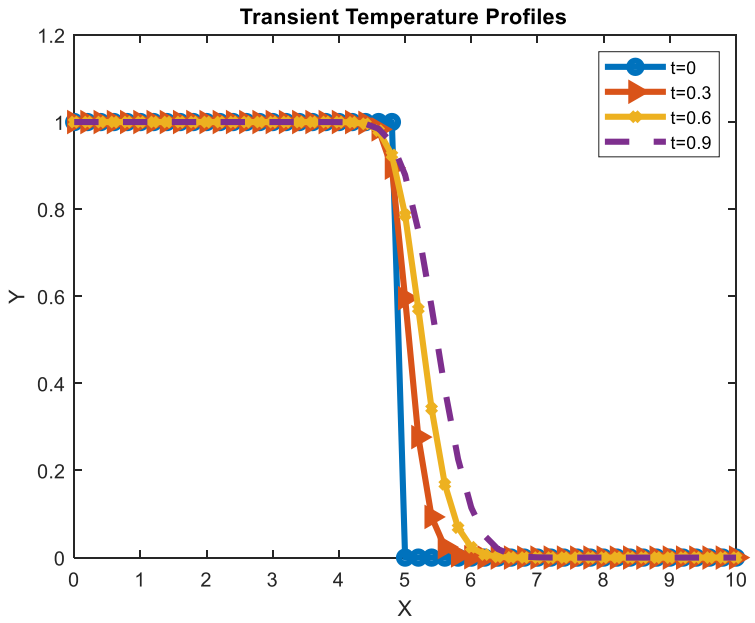

Fig. 8. Transient solution profiles for Example 3

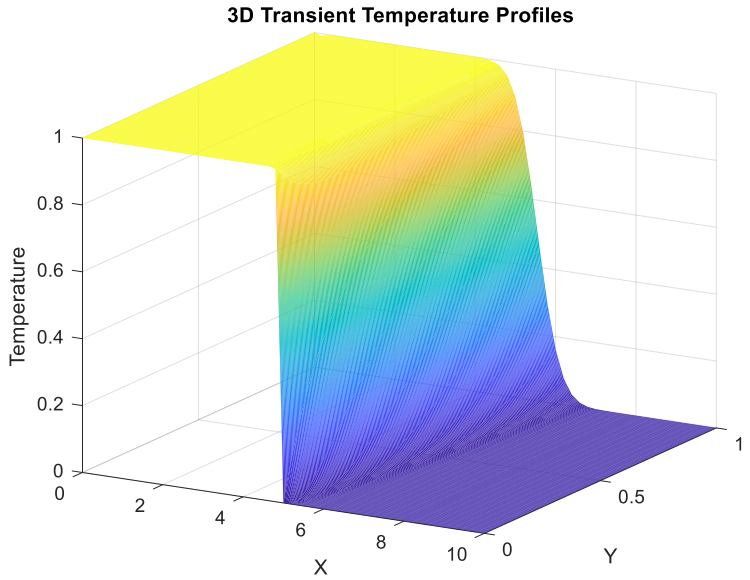

Fig. 9. 3D solution profiles for Example 3

2.4 Example 4

Consider the following IPDE

$$u_t = -2u^2 + 0.1u_{xx} + \int_0^t e^{-(t-s)/\tau} \quad u_{xx}(x,s)\,ds \tag{18}$$

where $(x,t)\in(0,50)\times(0,1]$. Initial condition: $u(x,0) = 8.1\sec h(x-25)^2$. Dirichlet and homogeneous boundary conditions: $u(0,t) = 0, \quad u(50,t) = 0$.

Figures 10 and 11 obtained herein are found to be in good agreement with those in [15] and example 2 of [24]. It can be seen that not only do the solutions decay with time; they all attain an apogee at $x \approx 25$ for both diagrams in agreement with the specified initial condition.

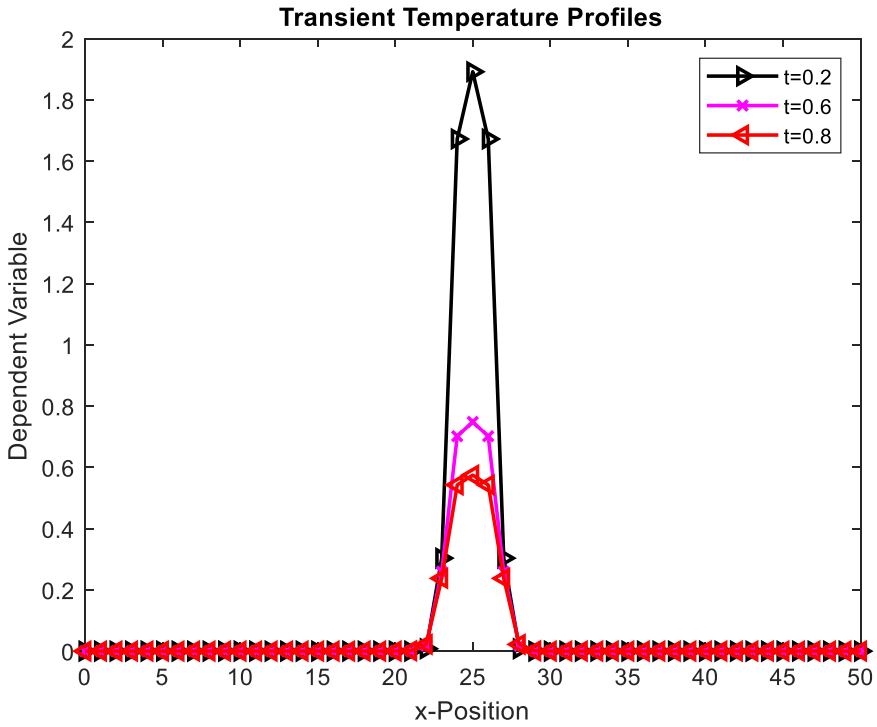

Fig. 10. Transient solution profiles for Example 4

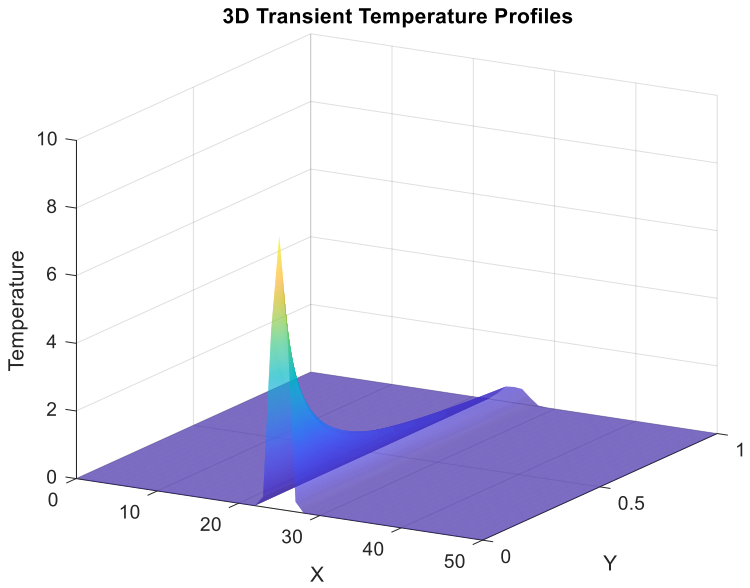

Fig. 11. 3D solution profiles for Example 4

4. Conclusions

In this work, we have applied a straightforward technique to solve nonlinear integro-differential partial differential equations with diffusion type integral kernels and different boundary conditions. Results obtained are in agreement with those found in literature. Numerical experiments carried out support high accuracy as evidenced by comparing numerical and analytic solutions as well as the ability to effectively handle the delayed response of the diffusion process to changes in scalar gradient. This further confirms that our approach apart from its simplicity and applicability is able to handle transport processes that incorporates a 'memory' of the systems past behavior. Despite a better understanding of this process a lot of work still needs to be done in areas involving high-viscosity fluids, nano fluids, biological systems involving transport in porous and heterogeneous media as well as electrochemical measurements.

References

[1] Roniotis, Alexandros, Kostas Marias, Vangelis Sakkalis, and Michalis Zervakis. "Diffusive modelling of glioma evolution: a review." Journal of Biomedical Science and Engineering 3, no. 05 (2010): 501. https://doi.org/10.4236/jbise.2010.35070

[2] Fakharany, Mohamed, R. Company, and Lucas Jódar. "Positive finite difference schemes for a partial integro-differential option pricing model." *Applied Mathematics and Computation* 249 (2014): 320-332. https://doi.org/10.1016/j.amc.2014.10.064

[3] Tabata, Minoru, Nobuoki Eshima, and Ichiro Takagi. "The nonlinear integro-partial differential equation describing the logistic growth of human population with migration." *Applied Mathematics and Computation* 98, no. 2-3 (1999): 169-183. https://doi.org/10.1016/S0096-3003(97)10172-2

[4] Fakhari, Hoorieh, and Akbar Mohebbi. "Galerkin spectral and finite difference methods for the solution of fourth-order time fractional partial integro-differential equation with a weakly singular kernel." *Journal of Applied Mathematics and Computing* 70, no. 5 (2024): 5063-5080. https://doi.org/10.1007/s12190-024-02173-6

[5] Dehestani, Haniye, and Yadollah Ordokhani. "An efficient approach based on Legendre–Gauss–Lobatto quadrature and discrete shifted Hahn polynomials for solving Caputo–Fabrizio fractional Volterra partial integro-differential equations." *Journal of Computational and Applied Mathematics* 403 (2022): 113851. https://doi.org/10.1016/j.cam.2021.113851

[6] Fakharany, M., Mahmoud M. El-Borai, and M. A. Abu Ibrahim. "Numerical analysis of finite difference schemes arising from time-memory partial integro-differential equations." Frontiers in Applied Mathematics and Statistics 8 (2022): 1055071. https://doi.org/10.3389/fams.2022.1055071

[7] Fakharany, M., Mahmoud M. El-Borai, and MA Abu Ibrahim. "A unified approach to solving parabolic Volterra partial integro-differential equations for a broad category of kernels: Numerical analysis and computing." *Results in Applied Mathematics* 21 (2024): 100425. https://doi.org/10.1016/j.rinam.2023.100425

[8] Qiao, Leijie, Zhibo Wang, and Da Xu. "An ADI finite difference method for the two-dimensional Volterra integro-differential equation with weakly singular kernel." *International Journal of Computer Mathematics* 99, no. 12 (2022): 2542-2554. https://doi.org/10.1080/00207160.2022.2073178

[9] Fakhari, Hoorieh, and Akbar Mohebbi. "Galerkin spectral and finite difference methods for the solution of fourth-order time fractional partial integro-differential equation with a weakly singular kernel." *Journal of Applied Mathematics and Computing* 70, no. 5 (2024): 5063-5080. https://doi.org/10.1007/s12190-024-02173-6

[10] Abbaszadeh, Mostafa, and Mehdi Dehghan. "A finite-difference procedure to solve weakly singular integro partial differential equation with space-time fractional derivatives." *Engineering with computers* 37 (2021): 2173-2182. https://doi.org/10.1007/s00366-020-00936-w

[11] Amer, Y. A., A. M. S. Mahdy, and E. S. M. Youssef. "Solving fractional integro-differential equations by using Sumudu transform method and Hermite spectral collocation method." *Computers, Materials and Continua* 54, no. 2 (2018): 161-180. https://doi.org/10.3970/cmc.2018.054.161

[12] Yüzbaşı, Şuayip, and Gamze Yıldırım. "A collocation method to solve the parabolic-type partial integro-differential equations via Pell–Lucas polynomials." *Applied Mathematics and Computation* 421 (2022): 126956. https://doi.org/10.1016/j.amc.2022.126956

[13] Taghipour, Mehran, and Hossein Aminikhah. "A fast collocation method for solving the weakly singular fractional integro-differential equation." *Computational and Applied Mathematics* 41, no. 4 (2022): 142. https://doi.org/10.1007/s40314-022-01845-y

[14] Adewole, Matthew Olayiwola. "Finite element solution of a class of parabolic integro-differential equations with inhomogeneous jump conditions using FreeFEM++." *Computational Methods for Differential Equations* 12, no. 2 (2024): 314-328. https://doi.org/10.22034/cmde.2023.50871.2114

[15] Khuri, Suheil A., and Ali Sayfy. "A numerical approach for solving an extended Fisher–Kolomogrov–Petrovskii–Piskunov equation." *Journal of computational and applied mathematics* 233, no. 8 (2010): 2081-2089. https://doi.org/10.1016/j.cam.2009.09.041

[16] Jiang, Y.J., 2009. On spectral methods for Volterra-type integro-differential equations. *Journal of computational and applied mathematics*, *230*(2), pp.333-340. https://doi.org/10.1016/j.cam.2008.12.001

[17] Zheng, Weishan, Yanping Chen, and Jianwei Zhou. "A Legendre spectral method for multidimensional partial Volterra integro-differential equations." *Journal of Computational and Applied Mathematics* 436 (2024): 115302. https://doi.org/10.1016/j.cam.2023.115302

[18] Liu, ZhiPeng, DongYa Tao, and Chao Zhang. "An efficient spectral method for nonlinear Volterra integro-differential equations with weakly singular kernels." *Mathematical Modelling and Analysis* 29, no. 3 (2024): 387-405. https://doi.org/10.3846/mma.2024.18354

[19] Zhang, Chao, Zhipeng Liu, Sheng Chen, and DongYa Tao. "New spectral element method for Volterra integral equations with weakly singular kernel." Journal of Computational and Applied Mathematics 404 (2022): 113902. https://doi.org/10.1016/j.cam.2021.113902

[20] Zheng, Weishan, and Yanping Chen. "A spectral method for a weakly singular Volterra integro-differential equation with pantograph delay." *Acta Mathematica Scientia* 42, no. 1 (2022): 387-402. https://doi.org/10.1007/s10473-022-0121-0

[21] Ferreira, Jose A., and Luis Pinto. "An integro-differential model for non-Fickian tracer transport in porous media: validation and numerical simulation." *Mathematical Methods in the Applied Sciences* 39, no. 16 (2016): 4736-4749. https://doi.org/10.1002/mma.3446

[22] Branco, J. R., and J. A. Ferreira. "A singular perturbation of the heat equation with memory." *Journal of computational and applied mathematics* 218, no. 2 (2008): 376-394. https://doi.org/10.1016/j.cam.2007.04.007

[23] Li, Dongfang, Chengjian Zhang, and Wansheng Wang. "Long time behavior of non-Fickian delay reaction–diffusion equations." *Nonlinear Analysis: Real World Applications* 13, no. 3 (2012): 1401-1415. https://doi.org/10.1016/j.nonrwa.2011.11.005

[24] Araújo, A., J. R. Branco, and J. A. Ferreira. "On the stability of a class of splitting methods for integro-differential equations." *Applied Numerical Mathematics* 59, no. 3-4 (2009): 436-453. https://doi.org/10.1016/j.apnum.2008.03.005